HHS Public Access

Author manuscript

Mol Cancer Res. Author manuscript; available in PMC 2020 December 19.

Published in final edited form as:

Mol Cancer Res. 2020 July ; 18(7): 1039–1049. doi:10.1158/1541-7786.MCR-19-1104.

Iron Regulatory Protein 2 Exerts its Oncogenic Activities by Suppressing TAp63 Expression

Yanhong Zhang[1], **Xiuli Feng**[1,2], **Jin Zhang**[1], **Xinbin Chen**[1]

[1]Comparative Oncology Laboratory, Schools of Veterinary Medicine and Medicine, University of California at Davis, Davis, California.

[2]College of Veterinary Medicine, Nanjing Agricultural University, Nanjing, China.

Abstract

Iron regulatory protein 2 (IRP2) is a key regulator of iron homeostasis and is found to be altered in several types of human cancer. However, how IRP2 contributes to tumorigenesis remains to be elucidated. In this study, we sought to investigate the role of IRP2 in tumorigenesis and found that IRP2 promotes cell growth by repressing TAp63, a member of p53 tumor suppressor family. Specifically, we found that IRP2 overexpression decreased, whereas *IRP2* deficiency increased, TAp63 expression. We also showed that the repression of TAp63 by IRP2 was independent of tumor suppressor p53. To uncover the molecular basis, we found that IRP2 stabilized *TAp63* mRNA by binding to an iron response element in the 3′UTR of *p63* mRNA. To determine the biological significance of this regulation, we showed that IRP2 facilitates cell proliferation, at least in part, via repressing TAp63 expression. Moreover, we found that *IRP2* deficiency markedly alleviated cellular senescence in *TAp63*-deficient mouse embryo fibroblasts. Together, we have uncovered a novel regulation of TAp63 by IRP2 and our data suggest that IRP2 exerts its oncogenic activities at least in part by repressing TAp63 expression.

Implications: We have revealed a novel regulation of *TAp63* by IRP2 and our data suggest that IRP2 exerts its oncogenic activities, at least in part, by repressing TAp63 expression.

Introduction

Iron is essential for all organisms. It is required by variety of proteins involved in cell growth and proliferation. Notably, recent studies showed that dysregulation of iron metabolism frequently occurs in cancer cells and contributes to cancer development. At the cellular level,

Corresponding Author: Xinbin Chen, University of California, Davis, 2128 Tupper Hall, VM: Surgical and Radiological Sciences, Davis, CA 95616. Phone: 530-754-8404; Fax: 530-752-6042; xbchen@ucdavis.edu.

Authors' Contributions

Conception and design: Y. Zhang, J. Zhang, X. Chen

Development of methodology: Y. Zhang

Acquisition of data (provided animals, acquired and managed patients, provided facilities, etc.): Y. Zhang, X. Feng

Analysis and interpretation of data (e.g., statistical analysis, biostatistics, computational analysis): Y. Zhang, J. Zhang, X. Chen

Writing, review, and/or revision of the manuscript: Y. Zhang, J. Zhang, X. Chen

Administrative, technical, or material support (i.e., reporting or organizing data, constructing databases): Y. Zhang, X. Chen

Study supervision: Y. Zhang, X. Chen

Note: Supplementary data for this article are available at Molecular Cancer Research Online (http://mcr.aacrjournals.org/).

Disclosure of Potential Conflicts of Interest

No potential conflicts of interest were disclosed.

the uptake, storage, and usage of iron are tightly governed by iron regulatory protein 1 (IRP1) and IRP2 (also known as ACO1 and IREB2, respectively; refs. 1, 2). IRP1 and IRP2 are cytosolic RNA-binding proteins that bind to iron-responsive elements (IRE) in their target mRNAs and regulate the translation or stability of mRNAs encoding proteins involved in cellular iron homeostasis (3–7). IRP1/2 repress mRNA translation when bound to an IRE located at the 5′UTR, including the ones coding for ferritin L (FTL) and H (FTH1; ref. 8), ALAS2 (9), ferroportin (SLC40A1; ref. 10), mitochondrial aconitase ACO2 and SDH (11), and HIF2α (12). In contrast, IRP1/2 regulate the stability of their target mRNAs through interaction with IREs in the 3′UTR, including the ones coding for TFR1 (8), SLC11A2 (9), CDC14A (13), Cdc42-binding kinase alpha (CDC42BPA; ref. 14) and glycolate oxidase (Hao1; ref. 15). The biological function of IRPs in regulating cellular iron metabolism has been confirmed in mouse models. Loss of *Irp2* in mouse models results in microcytic anemia, altered body iron distribution, and adult-onset progressive neurode-generation (16, 17). *IRP1* deficiency was initially found to be asymptomatic in mice (18), but later found to result in age-dependent erythropoietic abnormalities and dysregulation of body iron metabolism (19, 20). Despite the well-established role of IRP1/2 in iron metabolism, very little is known about their role in tumorigenesis.

p63 belongs to the p53 tumor suppressor family, including p53, p63, and p73 (21). Because of differential promoter usage and splicing, the *TP63* gene produces multiple isoforms: two N-terminal isoforms (TA and ΔN) and five C-terminal isoforms (α, β, γ, δ, ε; refs. 21, 22). All *TP63* isoforms contain an identical DNA-binding domain (DBD) and an oligomerization domain and are able to transactivate some p53 target genes related to tumor suppression, such as *CDKN1A (p21)* and *Bax* (21, 23). However, some *TP63* isoforms contain one or both unique domains at their C termini: sterile alpha motif and transcription-inhibitory domain, both of which can modulate target gene specificity (24–26). The biological function of TP63 has been explored in multiple studies with various mouse models. For example, loss of all *TP63* isoforms leads to aberrant epithelial development (21, 27). Interestingly, mice deficient in *TAp63* are tumor prone and display features of accelerated aging (28, 29). In contrast, mice deficient in Δ*Np63* have developmental defects, which resemble the phenotypes of total *TP63* knockout mice (30). These data suggest that *TP63* has a profound role in development, tumor suppression, and aging.

Because of the critical role of *TP63* in modulating various cellular processes, *TP63* expression is tightly controlled, which is mainly through posttranscriptional levels (31, 32). For example, c-Ab1, IKKβ, ATM, CDK2, and p38 can regulate *TP63* activity through protein phosphorylation and stability (33–36). Both ΔNp63 and mutant p53 can inactivate TAp63 in a dominant negative fashion (21, 37, 38). Our group found that *TP63* can be regulated via mRNA stability by Rbm24 and Rbm38 RNA-binding proteins (39–42). We and others also found that *TP63* is regulated by several miRNAs (41, 43, 44). However, whether *TP63* is regulated by other RNA-binding proteins remains unclear.

Among all three p53 family members, p53 has been found to play a role in iron metabolism as well as ferroptosis, an iron-mediated cell death (45). However, it is not certain whether other p53 family members play a role in iron metabolism. In this study, we sought to determine whether TAp63 is regulated by IRP2 and the biological significance of this

regulation. Indeed, we made novel observations that ectopic expression of IRP2 decreases, whereas IRP2 deficiency increases, p63 expression. We also found that IRP2 promotes cell proliferation at least in part via suppressing TAp63 expression. Furthermore, we found that loss of *IRP2* inhibits *TAp63* deficiency-induced cellular senescence. Together, our data suggest that IRP2 exerts its oncogenic activity via suppressing TAp63 expression and that the IRP2–p63 pathway may be explored as a cancer therapeutic strategy.

Materials and Methods

IRP2- and *TAp63*-mutant mouse models

Irp2$^{+/-}$ mice (ID: MMRRC: 030490-MU, on a C57BL/6N background) were obtained from Mutant Mouse Resource and Research Center (MMRRC) at the University of Missouri (Columbia, MO). The *TAp63*$^{+/-}$ mice on C57BL/6 background were kindly provided by Dr. E. Flores' laboratory (46). All animals were housed in a specific pathogen-free environment at the University of California, Davis (Davis, CA). The procedures for all animal experiments were approved by the Institutional Animal Care and Use Committee at University of California, Davis (Davis, CA).

Mouse embryonic fibroblasts' isolation

Irp2$^{+/-}$;*TAp63*$^{+/-}$ mice were intercrossed to generate ~13.5-day embryos, which were then used to isolate WT, *TAp63*$^{+/-}$, *Irp2*$^{-/-}$ and *Irp2*$^{-/-}$;*TAp63*$^{+/-}$ MEFs as described previously (47).

Cell culture

MIA-PaCa2, HepG2, Huh7, and Hep3B cells were originally purchased from the ATCC. The cell lines and their derivatives were cultured in DMEM (Invitrogen) supplemented with 10% FBS (Hyclone). Because these cell lines were authenticated and tested free for *Mycoplasma* by ATCC, no further authentication and *Mycoplasma* testing were performed, especially considering that these cell lines at low passages were used.

Plasmid construction and cell line generation

Cells deficient in *IRP2* or *p53* were generated and confirmed as described previously (48). The primers used to generate sgRNA expression vectors were listed in Supplementary Table S1. The primers used for genotyping cell lines were listed in Supplementary Table S2.

The pcDNA3–5′UTR-TAp63, pcDNA3-TAp63-CDS and pcDNA3-TAp63–3′UTR expression vectors were generated as described previously (40). pcDNA3 vector expressing GFP was generated as described previously (49). The 5′UTR-GFP and GFP-3′UTR reporters were generated by cloning p63 5′UTR or 3′UTR into pcDNA3-GFP downstream of GFP. p63 5′UTR was amplified with forward primer, 5′-AAG CTT CCC GGC TTT ATA TCT ATA TA-3′, and reverse primer, 5′-GGA TCC TTC CTT CAA CTG TCT TTG A-3′. p63 3′UTR was amplified as described previously (41). To generate pcDNA3-GFP-TAp63-ΔIRE, which lacks an IRE site (CAGUGU) at nt 2792, a two-step PCR strategy was used and pcDNA3-p63-3′UTR was used as a template. Fragment 1 was amplified with forward primer, 5′-CTC GAG GCC TCA CCA TGT GAG CTC-3′, and reverse primer, 5′-ATA

AAA TAT ACC AAG AAA AGA ATA CAT-3′. Fragment 2 was amplified with forward primer, 5′-ATG TAT TCT TTT CTT GGT TAT ATT TTA T-3′, and reverse primer, 5′-TCT AGA GCA TGT CCT GGC AAA CAA AAA G-3′. The second-step PCR was performed with forward primer, 5′-CTC GAG GCC TCA CCA TGT GAG CTC-3′, and reverse primer, 5′-TCT AGA GCA TGT CCT GGC AAA CAA AAA G-3′. The resulting PCR fragment was then cloned into pcDNA3-GFP vector to generate pcDNA3-GFP-p63–3′UTR-ΔIRE.

Western blot analysis

Western blot was performed as previously described (48). Antibodies against TAp63, p130, PML, IRP2, and actin were purchased from Santa Cruz Biotechnology. Anti-mouse IRP2 antibody was kindly gifted from Professor E. Leibold (University of Utah, Salt Lake City, UT; ref. 50).

RNA isolation, RT-PCR analysis, and qRT-PCR

Total RNA isolation, cDNA synthesis, and RT-PCR measurement of p63 and actin transcripts with the primers were performed as described previously (41).

RNA-chromatin immunoprecipitation assay

RNA-chromatin immunoprecipitation (RNA-ChIP) was carried out as described previously (51). RT–PCR analysis was performed to determine the level of RNA transcripts associated with IRP2. The primers for human *TFR* were as follows: forward primer, 5′-ACG CCA GAC TTT GCT GAG TT-3′; reverse primer, 5′-GAG GAG CCA GGA GAG GAC TT-3′. The primers for human *TAp63* were as follows: forward primer, 5′-TTA TTA CCG ATC CAC CAT GTC-3′; reverse primer, 5′-TGC GGA TAC AGT CCA TGC TA-3′. The primers used to amplify human *actin* were as follows: forward primer, 5′-CTG AAG TAC CCC ATC GAG CAC GGC A-3′; reverse primer, 5′-GGA TAG CAC AGC CTG GAT AGC AAC G-3′.

RNA interference

Scrambled siRNA (5′-GCA GUG UCU CCA CGU ACU AdTdT-3′), siRNAs against *IRP2* (si*IRP2*#1:5′-GCG AUU UCC AGG CUU GCU UdTdT −3′ and #2: 5′-GCA AAC AUG UGU CCG GAA dTdT-3′), and siRNA against human *TAp63* (5′-GAU GGU GCG ACA AAC AAG AdTdT-3′) were purchased from Dharmacon. For siRNA transfection, RNAiMax Lipid Reagent (Thermo Fisher Scientific) was used according to the manufacturer's manual. The siRNAs were transfected into the cells at the final concentration of 30 nmol/L for 3 days.

Colony formation assay

Colony formation assay was performed with HepG2, Hep3B, or their derivatives (1,000 cells per well) in 6-well plates for two weeks. Fixation and staining for colonies were performed as described previously (48). The density of colonies was scanned and analyzed using Image J (52).

Statistical analysis

The data were presented as mean ± SD. Statistical significance was determined by two-tailed Student *t* test. Values of $P < 0.05$ were considered significant.

Results

Ectopic expression of *IRP2* represses, whereas knockdown or knockout of *IRP2* increases, TAp63 expression regardless of p53 status

To test whether IRP2 regulates *TP63*, *IRP2* was ectopically expressed in HepG2 (carrying WT p53), Hep3B (p53-null), and MIA-PaCa2 (carrying mutant p53) cells. We showed that the levels of TAp63α protein were significantly reduced by ectopic expression of *IRP2* (Fig. 1A, C, and E). We also showed that the level of *TAp63* transcript was decreased by ectopic expression of *IRP2* (Fig. 1B, D, and F). To confirm this, *IRP2* was knocked down by two siRNAs that target different regions of *IRP2* mRNA (Fig. 2A, si*IRP2*#1 and si*IRP2*#2) in Hep3B cells. We showed that the level of TAp63α protein was reduced by silencing of *IRP2* (Fig. 2A). We also showed that the level of *TAp63* transcript was increased by silencing of *IRP2* (Fig. 2B and C). To further confirm this, we generated multiple *IRP2*-deficient cell lines by CRISPR/Cas9 from HepG2 (clone #35 and #57), MIA-PaCa2 (clone #8 and #46) and Huh7 (carrying mutant p53, clone #28 and #54) cells. We found that the level of TAp63 protein was much higher in $IRP2^{-/-}$ cells than that in isogenic control cells (Fig. 2D, G, and J). We also found that the level of *TAp63* transcript was increased in $IRP2^{-/-}$ cells (Fig. 2E and F, H and I, K and L). These data indicate that IRP2 represses TAp63 expression regardless of p53 status.

IRP2 regulates p63 expression via mRNA stability

Because IRP2 regulates p63 expression by altering the level of *TP63* transcript, we next determined whether *TP63* mRNA stability is regulated by IRP2. To test this, isogenic control and $IRP2^{-/-}$ MIA-PaCa2 cells were treated with 5,6-dichlorobenzimidazole-β-D-ribofuranoside (DRB; 100 μmol/L) to inhibit *de novo* RNA synthesis. We found that knockout of *IRP2* increased the half-life of *TAp63* mRNA from approximately 2.55 hours in isogenic control cells to approximately 3.58 hours in $IRP2^{-/-}$ cells (Fig. 3A). As a RNA-binding protein, we hypothesized that IRP2 might bind to *TP63* mRNA and then regulate p63 expression. To test this, RNA-ChIP assay was performed and showed that *p63* transcript was detected in IRP2-immunocomplexes from isogenic control cells, but little if any from *IRP2*-KO cells (Fig. 3B, compare lanes 5 and 6). We also showed that IRP2 bound to *TFR* mRNA, which is known to be recognized by *IRP2* but not *actin* mRNA (Fig. 3B, compare lanes 5 and 6).

Next, several reporters were generated to determine whether a region in *TP63* mRNA can be recognized by and responsive to IRP2 (Fig. 3C). We found that ectopic expression of *IRP2* decreased the level of p63 protein upon cotransfection with reporter expressing p63 CDS plus its 3′UTR in $IRP2^{-/-}$ MIA-PaCa2 cells (Fig. 3D, compare lanes 5 and 6). However, IRP2 could not alter p63 expression upon cotransfection with reporters expressing p63 CDS alone or together with p63 5′UTR (Fig. 3D, compare lane 1 and 3 with 2 and 4, respectively). To verify this, GFP expression vectors that carry GFP alone or together with

5′ or 3′UTR of p63 mRNA was generated (Fig. 3C). Consistently, we observed that loss of *IRP2* led to an increased GFP expression upon transfection with reporter expressing GFP CDS plus p63 3′UTR in MIA-PaCa2 cells (Fig. 3E, lanes 5 and 6). However, loss of *IRP2* could not alter GFP expression upon transfection with reporters expressing GFP CDS alone or together with p63 5′UTR reporter (Fig. 3E, lanes 1–4). As an internal control, we showed that endogenous p63 expression in MIA-PaCa2 cells was increased by *IRP2*-KO regardless of the overexpression of GFP reporters (Fig. 3E). Because p63 3′UTR is responsive to IRP2 (Fig. 3D and E), we searched for a conserved IRE consensus sequence consist of six-membered (CAGUGX) loop that can be recognized by IRP2 (53, 54). Interestingly, we located a putative IRE (CAGUGU) at nt 2792 in p63 3′UTR (Fig. 3C). We thus generated a GFP reporter harboring p63 3′UTR but lacks of such a putative IRE (Fig. 3C). We showed that IRP2 inhibited GFP expression upon transfection with a reporter that contains an intact p63 3′UTR in *IRP2*$^{-/-}$ MIA-PaCa2 cells (Fig. 3F, compare lanes 3 and 4). In contrast, IRP2 had no effect on GFP expression upon cotransfection with a reporter expressing IRE-deleted p63 3′UTR (Fig. 3F, compare lanes 5 and 6). As an internal control, we showed that endogenous p63 expression was reduced by ectopic expression of *IRP2* regardless of the transfection with a GFP reporter in *IRP2*$^{-/-}$ cells (Fig. 3F).

Ectopic expression of *IRP2* promotes, whereas knockdown of *IRP2* inhibits, cell growth, at least in part, via repressing TAp63

Previously, we demonstrated that IRP2 represses p53 expression via mRNA translation (47, 48). As p53 is a potent suppressor of cell growth, it is necessary to examine the effect of IRP2-mediated TAp63 expression on cell growth in the absence of p53. In this regard, *p53*$^{-/-}$ HepG2 cell lines were generated by using CRISPR/Cas9. Next, *p53*$^{-/-}$ HepG2 cells were transiently transfected with an IRP2 expression vector along with a control vector or a vector expressing TAp63 (Fig. 4A). We found that upon ectopic expression of *IRP2*, the levels of ectopic and endogenous TAp63 protein were decreased (Fig. 4A, compare lane 2 with 1, lane 4 with 3, respectively), consistent with the above observation in Fig. 1. Next, colony formation assay was performed and found that ectopic *IRP2* enhanced, whereas ectopic *TAp63* inhibited, colony formation in *p53*$^{-/-}$ HepG2 cells (Fig. 4B, compare the 1st column with the 2nd and 3rd column, respectively). Interestingly, we found that the reduced colony numbers by ectopic *TAp63* can be increased by ectopic *IRP2*, suggesting that IRP2 facilitates cell growth via repressing TAp63 expression (Fig. 4B, compare the 4th column with the 1st and 2nd columns, respectively). Similar results were observed in *p53*$^{-/-}$ Hep3B cell (Fig. 4C and D).

To further confirm that IRP2 promotes cell growth via repressing TAp63, *p53*$^{-/-}$ HepG2 cells were transiently transfected with a scrambled siRNA or a siRNA against *IRP2*, *TAp63*, or both. We showed that the level of TAp63 protein was increased by silencing of *IRP2* in *p53*$^{-/-}$ HepG2 cells (Fig. 5A, compare lanes 2 and 4 with 1 and 3, respectively), consistent with the above observation in Fig. 2. However, the level of IRP2 was not altered by silencing of *TAp63* (Fig. 5A, compare lanes 3 and 4 with 1 and 2, respectively). Next, we performed colony formation assay and showed that silencing of *IRP2* decreased the number of colonies in *p53*$^{-/-}$ HepG2 (Fig. 5B, compare the 1st with the 2nd column). In contrast, the number of colonies was increased by silencing of *TAp63* (Fig. 5B, compare the 3rd with the 1st

column). Most importantly, the decreased colony formation by silencing of *IRP2* was increased by silencing of *TAp63*, reaching the level in control cells (Fig. 5B, compare the 4th column with the 1st and 2nd columns, respectively). Similar results were observed in $p53^{-/-}$ Hep3B cells (Fig. 5C and D). Together, these observations suggest that IRP2 is required for cell growth, at least in part, via repressing TAp63 expression.

Loss of *IRP2* inhibits cellular senescence induced by *TAp63* deficiency

To further explore the biological significance of IRP2-mediated TAp63 repression, we generated a cohort of WT, $TAp63^{+/-}$, $Irp2^{-/-}$ and $Irp2^{-/-}$;$TAp63^{+/-}$ MEFs. As expected, the level of IRP2 protein was not detectable in $Irp2^{-/-}$ and $Irp2^{-/-}$;$TAp63^{+/-}$ MEFs (Fig. 6A, compare lanes 3 and 4 with 1 and 2) and loss of *Irp2* resulted in an increase in *TAp63* transcript in $Irp2^{-/-}$ MEFs (Fig. 6B, compare lanes 1 and 3). We also found that the level of *TAp63* transcript in $TAp63^{+/-}$ MEFs was restored to near WT level by loss of *Irp2* (Fig. 6B, compare lane 4 with lanes 1 and 2, respectively). Next, SA-β-gal assay was performed and we found that the percentage of SA-β-gal–positive cells was markedly increased in $TAp63^{+/-}$ MEFs (63%) as compared with that in WT MEFs (21%; Fig. 6C), consistent with the previous reports (29, 39). However, loss of *Irp2* alone had little effect on cellular senescence in $Irp2^{-/-}$ MEFs (Fig. 6C, the 3rd column). Importantly, loss of *Irp2* markedly reduced the number of SA-β–positive cells from 63% in $TAp63^{+/-}$ MEFs to 23% in $Irp2^{-/-}$;$TAp63^{+/-}$ MEFs ($P < 0.05$; Fig. 6C). Furthermore, we analyzed the expression of p130 and PML, both of which are known to play a role in triggering the senescence process (55, 56). We found that the levels of p130 and PML were highly increased in $TAp63^{+/-}$ MEFs (Fig. 6D, compare lane 2 with 1), consistent with previous reports (57, 58). In contrast, the levels of p130 and PML increased in $TAp63^{+/-}$ MEFs were reduced to near WT levels in $Irp2^{-/-}$;$TAp63^{+/-}$ MEFs (Fig. 6D, compare lane 4 with lanes 1 and 2, respectively). Together, these data indicate that loss of *Irp2* restores TAp63 expression in $TAp63^{+/-}$ MEFs and consequently inhibits cellular senescence induced by loss of *TAp63*.

Discussion

Recent studies indicate that iron metabolism plays a critical role in contributing tumorigenesis. However, very little is known about the role of IRP2 in tumorigenesis despite its well-studied role in modulating iron homeostasis. In this study, we examined whether IRP2 regulates expression of TAp63, a member of p53 tumor suppressor family. We found that IRP2 represses TAp63 expression regardless of p53 status (Figs. 1 and 2), suggesting that TAp63 expression is regulated directly by IRP2 in a p53-independent manner. In addition, we found that IRP2 stabilizes *TAp63* mRNA stability via a putative IRE in p63 3′UTR (Fig. 3). We would like to note that p63 3′UTR is also recognized by and responsive to Rbm38 and Rbm24, both of which regulate p63 expression via mRNA stability (39–42). These data indicate that *TP63* mRNA stability is uniquely regulated by multiple RNA-binding proteins through its 3′UTR. Thus, further studies are warranted to determine whether these RNA-binding proteins can coordinate to regulate p63 expression.

In our study, we found that ectopic expression of IRP2 suppresses TAp63 expression and subsequently, promotes cell growth, the latter of which can be blocked by ectopic expression

of TAp63 (Fig. 4). In contrast, loss of *IRP2* increases TAp63 expression and subsequently, inhibits cell growth, the latter of which can be blocked by knockdown of *TAp63* (Fig. 5). These data suggest that IRP2 promotes cell growth, at least in part, via repressing TAp63 expression. A hypothesis is summarized in Fig. 6E. Nevertheless, several questions remain to be addressed. First, *in vivo* studies are needed to determine whether IRP2-mediated TAp63 repression is capable of promoting tumor formation. Second, as IRP2 functions as a key regulator of iron homeostasis, it would be interesting to determine whether IRP2-mediated TAp63 repression plays a role in iron metabolism, such as modulating the liable iron pool. Third, due to the usage of two different promoters, *TP63* is expressed as two isoforms, *TAp63* and Δ*Np63*, with opposing functions. As we showed that IRP2 stabilizes *TAp63* mRNA (Fig. 3), it is possible that IRP2 stabilizes Δ*Np63* mRNA due to the same 3′UTR. Thus, further studies are needed to examine the regulation of ΔNp63 by IRP2 and whether this regulation contributes to tumorigenesis.

It is known that cellular senescence is a tumor-suppressing mechanism but also leads to accelerated aging (59, 60). In our study, we showed that loss of *IRP2* alleviates cellular senescence mediated by *TAp63* deficiency (Fig. 6). Notably, several reports showed that dysfunctional iron homeostasis is associated with aging (61, 62). In addition, *TAp63*-deficient mice are prone to premature aging. Thus, it would be important to examine whether the IRP2–TAp63 axis plays a role in aging by altering iron metabolism.

In conclusion, our study revealed a novel regulation of TAp63 by IRP2 and our data indicate that IRP2 exerts its oncogenic activity at least partly via suppressing TAp63 expression. Given that TAp63 is capable of suppressing tumorigenesis (63), these observations prompt us to speculate that targeting IRP2 may be used to restore TAp63 expression, which can be explored as a cancer therapeutic strategy.

Supplementary Material

Refer to Web version on PubMed Central for supplementary material.

Acknowledgments

This work was supported in part by the NIH grants CA224433-01 and CA195828 and Center for Companion Animal Health (CCAH) Faculty Grants 2017-26-F, School of Veterinary Medicine, University of California, Davis.

References

1. Gray NK, Hentze MW. Iron regulatory protein prevents binding of the 43S translation pre-initiation complex to ferritin and eALAS mRNAs. EMBO J 1994; 13:3882–91. [PubMed: 8070415]
2. Pantopoulos K. Iron metabolism and the IRE/IRP regulatory system: an update. Ann N Y Acad Sci 2004;1012:1–13. [PubMed: 15105251]
3. Hentze MW, Seuanez HN, O'Brien SJ, Harford JB, Klausner RD. Chromosomal localization of nucleic acid-binding proteins by affinity mapping: assignment of the IRE-binding protein gene to human chromosome 9. Nucleic Acids Res 1989;17:6103–8. [PubMed: 2771641]
4. Rouault TA, Tang CK, Kaptain S, Burgess WH, Haile DJ, Samaniego F, et al. Cloning of the cDNA encoding an RNA regulatory protein–the human iron-responsive element-binding protein. Proc Natl Acad Sci U S A 1990;87:7958–62. [PubMed: 2172968]

5. Klausner RD, Rouault TA, Harford JB. Regulating the fate of mRNA: the control of cellular iron metabolism. Cell 1993;72:19–28. [PubMed: 8380757]
6. Leibold EA, Guo B. Iron-dependent regulation of ferritin and transferrin receptor expression by the iron-responsive element binding protein. Annu Rev Nutr 1992;12:345–68. [PubMed: 1323982]
7. Theil EC. The IRE (iron regulatory element) family: structures which regulate mRNA translation or stability. Biofactors 1993;4:87–93. [PubMed: 8347279]
8. Hentze MW, Rouault TA, Caughman SW, Dancis A, Harford JB, Klausner RD. A cis-acting element is necessary and sufficient for translational regulation of human ferritin expression in response to iron. Proc Natl Acad Sci U S A 1987;84:6730–4. [PubMed: 3477805]
9. Dandekar T, Stripecke R, Gray NK, Goossen B, Constable A, Johansson HE, et al. Identification of a novel iron-responsive element in murine and human erythroid delta-aminolevulinic acid synthase mRNA. EMBO J 1991;10:1903–9. [PubMed: 2050126]
10. McKie AT, Marciani P, Rolfs A, Brennan K, Wehr K, Barrow D, et al. A novel duodenal iron-regulated transporter, IREG1, implicated in the basolateral transfer of iron to the circulation. Mol Cell 2000;5:299–309. [PubMed: 10882071]
11. Gray NK, Pantopoulos K, Dandekar T, Ackrell BA, Hentze MW. Translational regulation of mammalian and Drosophila citric acid cycle enzymes via iron-responsive elements. Proc Natl Acad Sci U S A 1996;93:4925–30. [PubMed: 8643505]
12. Sanchez M, Galy B, Muckenthaler MU, Hentze MW. Iron-regulatory proteins limit hypoxia-inducible factor-2alpha expression in iron deficiency. Nat Struct Mol Biol 2007;14:420–6. [PubMed: 17417656]
13. Sanchez M, Galy B, Dandekar T, Bengert P, Vainshtein Y, Stolte J, et al. Iron regulation and the cell cycle: identification of an iron-responsive element in the 3′-untranslated region of human cell division cycle 14A mRNA by a refined microarray-based screening strategy. J Biol Chem 2006;281:22865–74. [PubMed: 16760464]
14. Cmejla R, Petrak J, Cmejlova J. A novel iron responsive element in the 3′UTR of human MRCKalpha. Biochem Biophys Res Commun 2006;341:158–66. [PubMed: 16412980]
15. Kohler SA, Menotti E, Kuhn LC. Molecular cloning of mouse glycolate oxidase. High evolutionary conservation and presence of an iron-responsive element-like sequence in the mRNA. J Biol Chem 1999;274:2401–7. [PubMed: 9891009]
16. Cooperman SS, Meyron-Holtz EG, Olivierre-Wilson H, Ghosh MC, McConnell JP, Rouault TA. Microcytic anemia, erythropoietic protoporphyria, and neuro-degeneration in mice with targeted deletion of iron-regulatory protein 2. Blood 2005;106:1084–91. [PubMed: 15831703]
17. Galy B, Ferring D, Minana B, Bell O, Janser HG, Muckenthaler M, et al. Altered body iron distribution and microcytosis in mice deficient in iron regulatory protein 2 (IRP2). Blood 2005;106:2580–9. [PubMed: 15956281]
18. Meyron-Holtz EG, Ghosh MC, Iwai K, LaVaute T, Brazzolotto X, Berger UV, et al. Genetic ablations of iron regulatory proteins 1 and 2 reveal why iron regulatory protein 2 dominates iron homeostasis. EMBO J 2004;23:386–95. [PubMed: 14726953]
19. Ghosh MC, Zhang DL, Jeong SY, Kovtunovych G, Ollivierre-Wilson H, Noguchi A, et al. Deletion of iron regulatory protein 1 causes polycythemia and pulmonary hypertension in mice through translational derepression of HIF2alpha. Cell Metab 2013;17:271–81. [PubMed: 23395173]
20. Anderson SA, Nizzi CP, Chang YI, Deck KM, Schmidt PJ, Galy B, et al. The IRP1-HIF-2alpha axis coordinates iron and oxygen sensing with erythropoiesis and iron absorption. Cell Metab 2013;17:282–90. [PubMed: 23395174]
21. Yang A, Kaghad M, Wang Y, Gillett E, Fleming MD, Dotsch V, et al. p63, a p53 homolog at 3q27–29, encodes multiple products with transactivating, death-inducing, and dominant-negative activities. Mol Cell 1998;2:305–16. [PubMed: 9774969]
22. Mangiulli M, Valletti A, Caratozzolo MF, Tullo A, Sbisa E, Pesole G, et al. Identification and functional characterization of two new transcriptional variants of the human p63 gene. Nucleic Acids Res 2009;37:6092–104. [PubMed: 19700772]
23. Moll UM, Slade N. p63 and p73: roles in development and tumor formation. Mol Cancer Res 2004;2:371–86. [PubMed: 15280445]

24. De Laurenzi V, Melino G. Evolution of functions within the p53/p63/p73 family. Ann N Y Acad Sci 2000;926:90–100. [PubMed: 11193045]
25. Melino G, Lu X, Gasco M, Crook T, Knight RA. Functional regulation of p73 and p63: development and cancer. Trends Biochem Sci 2003;28:663–70. [PubMed: 14659698]
26. Yang A, McKeon F. P63 and P73: P53 mimics, menaces and more. Nat Rev Mol Cell Biol 2000;1:199–207. [PubMed: 11252895]
27. Mills AA, Zheng B, Wang XJ, Vogel H, Roop DR, Bradley A. p63 is a p53 homologue required for limb and epidermal morphogenesis. Nature 1999;398: 708–13. [PubMed: 10227293]
28. Su X, Chakravarti D, Cho MS, Liu L, Gi YJ, Lin YL, et al. TAp63 suppresses metastasis through coordinate regulation of Dicer and miRNAs. Nature 2010;467:986–90. [PubMed: 20962848]
29. Su X, Paris M, Gi YJ, Tsai KY, Cho MS, Lin YL, et al. TAp63 prevents premature aging by promoting adult stem cell maintenance. Cell Stem Cell 2009;5:64–75. [PubMed: 19570515]
30. Romano RA, Smalley K, Magraw C, Serna VA, Kurita T, Raghavan S, et al. DeltaNp63 knockout mice reveal its indispensable role as a master regulator of epithelial development and differentiation. Development 2012;139:772–82. [PubMed: 22274697]
31. Armstrong SR, Wu H, Wang B, Abuetabh Y, Sergi C, Leng RP. The regulation of tumor suppressor p63 by the ubiquitin-proteasome system. Int J Mol Sci 2016;17;2041.
32. Rossi M, Aqeilan RI, Neale M, Candi E, Salomoni P, Knight RA, et al. The E3 ubiquitin ligase Itch controls the protein stability of p63. Proc Natl Acad Sci U S A 2006;103:12753–8. [PubMed: 16908849]
33. Gonfloni S, Di Tella L, Caldarola S, Cannata SM, Klinger FG, Di Bartolomeo C, et al. Inhibition of the c-Abl-TAp63 pathway protects mouse oocytes from chemotherapy-induced death. Nat Med 2009;15:1179–85. [PubMed: 19783996]
34. Hildesheim J, Belova GI, Tyner SD, Zhou X, Vardanian L, Fornace AJ Jr. Gadd45a regulates matrix metalloproteinases by suppressing DeltaNp63alpha and beta-catenin via p38 MAP kinase and APC complex activation. Oncogene 2004;23:1829–37. [PubMed: 14647429]
35. Huang Y, Sen T, Nagpal J, Upadhyay S, Trink B, Ratovitski E, et al. ATM kinase is a master switch for the Delta Np63 alpha phosphorylation/degradation in human head and neck squamous cell carcinoma cells upon DNA damage. Cell Cycle 2008;7:2846–55. [PubMed: 18769144]
36. MacPartlin M, Zeng SX, Lu H. Phosphorylation and stabilization of TAp63-gamma by IkappaB kinase-beta. J Biol Chem 2008;283:15754–61. [PubMed: 18411264]
37. Adorno M, Cordenonsi M, Montagner M, Dupont S, Wong C, Hann B, et al. A mutant-p53/Smad complex opposes p63 to empower TGFbeta-induced metastasis. Cell 2009;137:87–98. [PubMed: 19345189]
38. Stindt MH, Muller PA, Ludwig RL, Kehrloesser S, Dotsch V, Vousden KH. Functional interplay between MDM2, p63/p73 and mutant p53. Oncogene 2015; 34:4300–10. [PubMed: 25417702]
39. Jiang Y, Xu E, Zhang J, Chen M, Flores E, Chen X. The Rbm38-p63 feedback loop is critical for tumor suppression and longevity. Oncogene 2018;37:2863–72. [PubMed: 29520104]
40. Zhang J, Jun Cho S, Chen X. RNPC1, an RNA-binding protein and a target of the p53 family, regulates p63 expression through mRNA stability. Proc Natl Acad Sci U S A 2010;107:9614–9. [PubMed: 20457941]
41. Zhang Y, Feng X, Sun W, Zhang J, Chen X. Serine 195 phosphorylation in the RNA-binding protein Rbm38 increases p63 expression by modulating Rbm38's interaction with the Ago2-miR203 complex. J Biol Chem 2019; 294:2449–59. [PubMed: 30567739]
42. Xu E, Zhang J, Zhang M, Jiang Y, Cho SJ, Chen X. RNA-binding protein RBM24 regulates p63 expression via mRNA stability. Mol Cancer Res 2014;12:359–69. [PubMed: 24375645]
43. Lena AM, Shalom-Feuerstein R, Rivetti di Val Cervo P, Aberdam D, Knight RA, Melino G, et al. miR-203 represses 'stemness' by repressing DeltaNp63. Cell Death Differ 2008;15:1187–95. [PubMed: 18483491]
44. Mehrazarin S, Chen W, Oh JE, Liu ZX, Kang KL, Yi JK, et al. The p63 gene is regulated by grainyhead-like 2 (GRHL2) through reciprocal feedback and determines the epithelial phenotype in human keratinocytes. J Biol Chem 2015;290:19999–20008. [PubMed: 26085095]
45. Zhang J, Chen X. p53 tumor suppressor and iron homeostasis. FEBS J 2019;286:620–9. [PubMed: 30133149]

46. Su X, Gi YJ, Chakravarti D, Chan IL, Zhang A, Xia X, et al. TAp63 is a master transcriptional regulator of lipid and glucose metabolism. Cell Metab 2012;16: 511–25. [PubMed: 23040072]
47. Zhang Y, Qian Y, Zhang J, Yan W, Jung YS, Chen M, et al. Ferredoxin reductase is critical for p53-dependent tumor suppression via iron regulatory protein 2. Genes Dev 2017;31:1243–56. [PubMed: 28747430]
48. Zhang Y, Feng X, Zhang J, Chen M, Huang E, Chen X. Iron regulatory protein 2 is a suppressor of mutant p53 in tumorigenesis. Oncogene 2019;38:6256–69. [PubMed: 31332290]
49. Zhang M, Zhang J, Chen X, Cho SJ, Chen X. Glycogen synthase kinase 3 promotes p53 mRNA translation via phosphorylation of RNPC1. Genes Dev 2013;27:2246–58. [PubMed: 24142875]
50. Guo B, Yu Y, Leibold EA. Iron regulates cytoplasmic levels of a novel iron-responsive element-binding protein without aconitase activity. J Biol Chem 1994;269:24252–60. [PubMed: 7523370]
51. Peritz T, Zeng F, Kannanayakal TJ, Kilk K, Eiriksdottir E, Langel U, et al. Immunoprecipitation of mRNA-protein complexes. Nat Protoc 2006;1:577–80. [PubMed: 17406284]
52. Guzman C, Bagga M, Kaur A, Westermarck J, Abankwa D. ColonyArea: an ImageJ plugin to automatically quantify colony formation in clonogenic assays. PLoS One 2014;9:e92444. [PubMed: 24647355]
53. Butt J, Kim HY, Basilion JP, Cohen S, Iwai K, Philpott CC, et al. Differences in the RNA binding sites of iron regulatory proteins and potential target diversity. Proc Natl Acad Sci U S A 1996;93:4345–9. [PubMed: 8633068]
54. Henderson BR, Menotti E, Kuhn LC. Iron regulatory proteins 1 and 2 bind distinct sets of RNA target sequences. J Biol Chem 1996;271:4900–8. [PubMed: 8617762]
55. Helmbold H, Deppert W, Bohn W. Regulation of cellular senescence by Rb2/p130. Oncogene 2006;25:5257–62. [PubMed: 16936745]
56. Pearson M, Carbone R, Sebastiani C, Cioce M, Fagioli M, Saito S, et al. PML regulates p53 acetylation and premature senescence induced by oncogenic Ras. Nature 2000;406:207–10. [PubMed: 10910364]
57. Bernassola F, Oberst A, Melino G, Pandolfi PP. The promyelocytic leukaemia protein tumour suppressor functions as a transcriptional regulator of p63. Oncogene 2005;24:6982–6. [PubMed: 16007146]
58. McDade SS, Patel D, McCance DJ. p63 maintains keratinocyte proliferative capacity through regulation of Skp2-p130 levels. J Cell Sci 2011; 124:1635–43. [PubMed: 21511729]
59. Narita M, Lowe SW. Senescence comes of age. Nat Med 2005;11:920–2. [PubMed: 16145569]
60. Braig M, Lee S, Loddenkemper C, Rudolph C, Peters AH, Schlegelberger B, et al. Oncogene-induced senescence as an initial barrier in lymphoma development. Nature 2005;436:660–5. [PubMed: 16079837]
61. Xu J, Jia Z, Knutson MD, Leeuwenburgh C. Impaired iron status in aging research. Int J Mol Sci 2012;13:2368–86. [PubMed: 22408459]
62. Wawer AA, Jennings A, Fairweather-Tait SJ. Iron status in the elderly: a review of recent evidence. Mech Ageing Dev 2018;175:55–73. [PubMed: 30040993]
63. Westfall MD, Pietenpol JA. p63: Molecular complexity in development and cancer. Carcinogenesis 2004;25:857–64. [PubMed: 15033906]

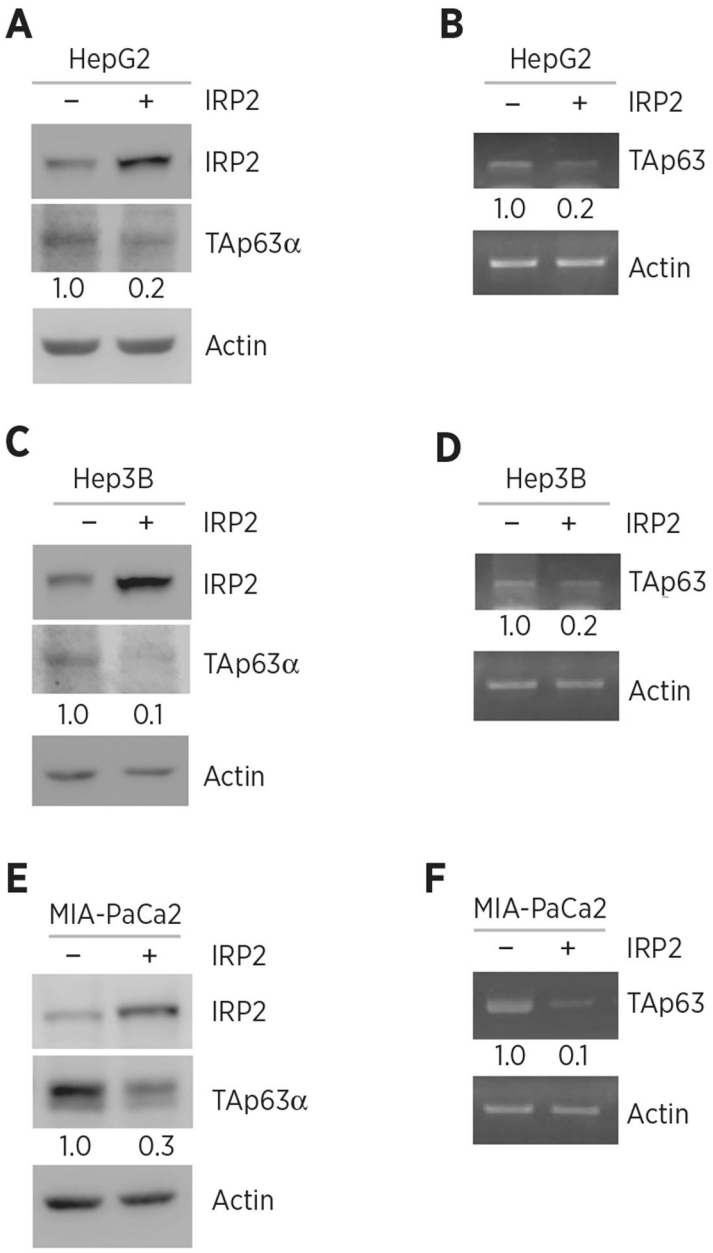

Figure 1.

Ectopic expression of *IRP2* represses TAp63 expression. **A,** HepG2 cells were transfected with a control vector or a vector expressing HA-tagged IRP2 for 24 hours. Cell lysates were collected and subjected to Western blot analysis with various antibodies as indicated. The level of proteins was normalized to that of actin, and the relative fold change is shown below each lane. **B,** The experiments were performed as in **A** except that the levels of TAp63 and actin transcripts were measured. The level of transcripts was normalized to that of actin, and the relative fold change is shown below each lane. **C** and **D,** The experiments were performed as in **A** and **B** except that Hep3B cells were used. **E** and **F,** The experiments were performed as in **A** and **B** except that MIA-PaCa2 cells were used.

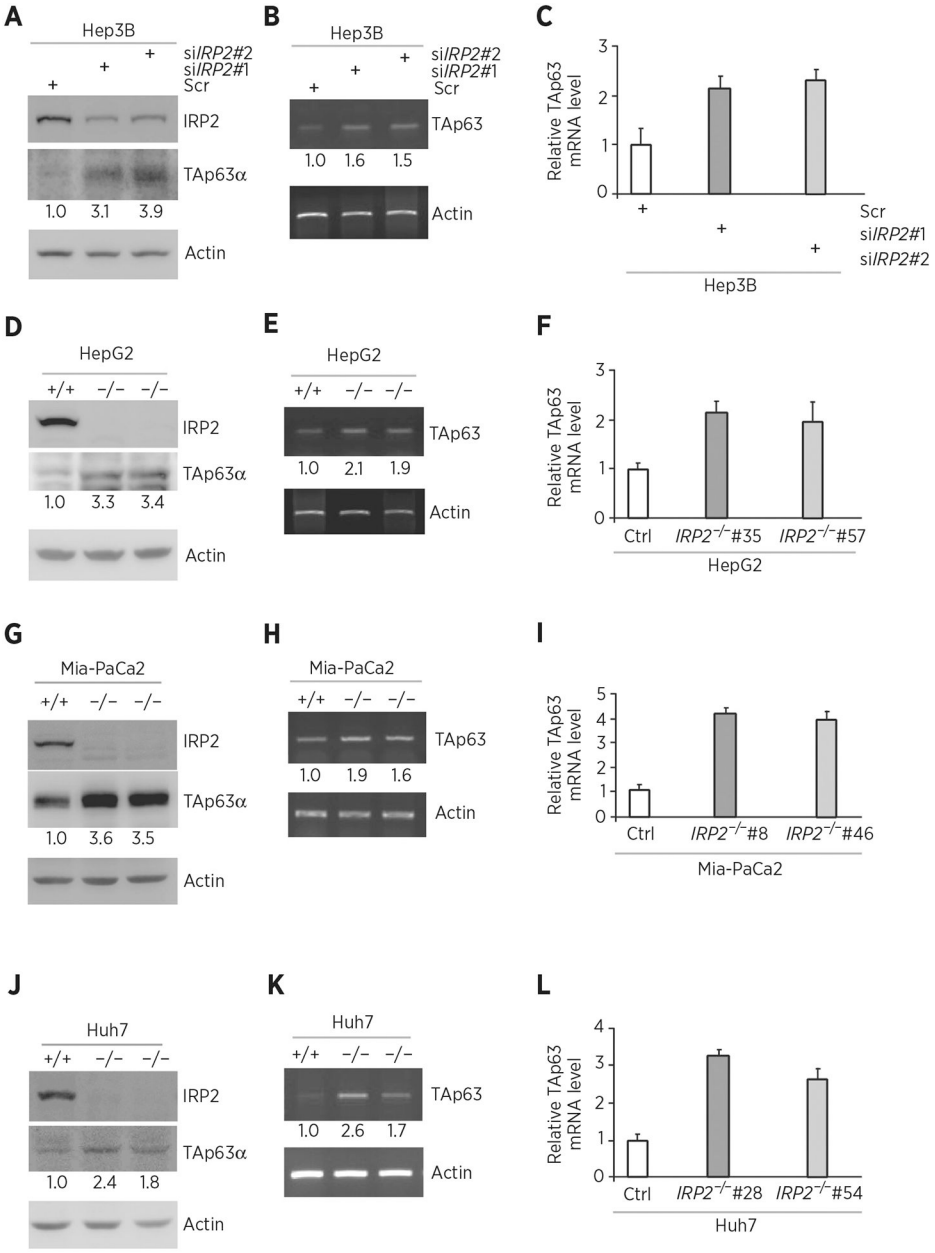

Figure 2.

Knockdown or knockout of *IRP2* increases p63 expression. **A,** Hep3B cells were transfected with scrambled siRNA (Scr) or siRNA against *IRP2* for 72 hours. Cell lysates were collected and subjected to Western blot analysis with various antibodies as indicated. The level of proteins was normalized to that of actin, and the relative fold change is shown below each lane. **B,** The levels of *TAp63* and *actin* transcripts were measured in Hep3B cells transfected with scrambled siRNA or siRNA against *IRP2* for 72 hours. The level of transcripts was normalized to that of actin, and the relative fold change is shown below each lane. **C,** Quantitative RT-PCR was performed to measure the levels of TAp63 transcripts in Hep3B cells transfected with scrambled siRNA or siRNA against *IRP2* for 72 hours. **D,** Western blots were prepared with lysates from isogenic control or *IRP2*$^{-/-}$ HepG2 cells, and then

probed with antibodies against IRP2, *TAp63*α, and *actin*, respectively. The level of proteins was normalized to that of actin, and the relative fold change is shown below each lane. **E,** The levels of TAp63 and actin transcripts were measured in isogenic control or *IRP2*$^{-/-}$ HepG2 cells. The level of transcripts was normalized to that of actin, and the relative fold change is shown below each lane. **F,** Quantitative RT-PCR was performed to measure the levels of *TAp63* transcripts in isogenic control or *IRP2*$^{-/-}$ HepG2 cells. **G–I,** The experiments were performed as in **D–F** except that isogenic control or *IRP2*$^{-/-}$ MIA-PaCa2 cells were used. **J–L,** The experiments were performed as in **D–F** except that isogenic control or *IRP2*$^{-/-}$ Huh7 cells were used.

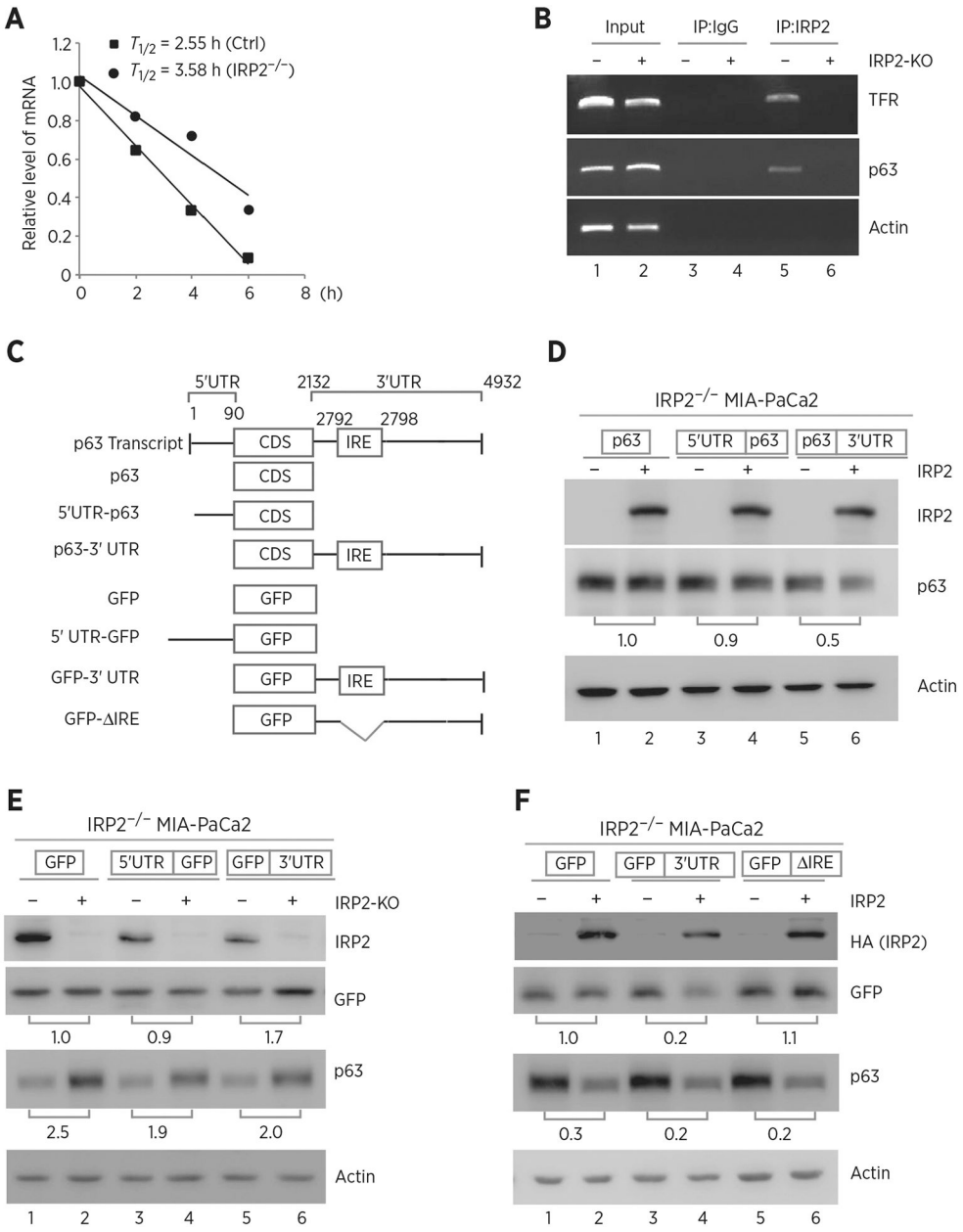

Figure 3.

IRP2 regulates *TP63* mRNA stability. **A,** The half-life of *TP63* mRNA was determined in isogenic control or *IRP2*$^{-/-}$ MIA-PaCa2 cells. The level of *TAp63* transcript was measured by qRT-PCR in isogenic control or *IRP2*$^{-/-}$ MIA-PaCa2 cells treated with 5,6-dichlorobenzimidazole-β-D-ribofuranoside (DRB; 100 μmol/L) for various times. mRNA was normalized by level of actin mRNA from triplicate samples and presented as mean ± SD. **B,** RNA-ChIP was performed with DNAase I–treated extracts from isogenic control (−) or *IRP2*$^{-/-}$ (+) MIA-PaCa2 cells with control IgG or anti-IRP2. Total RNAs were purified from immunocomplexes and subjected to RT-PCR to measure the levels of IRP2, p63, TFR and actin mRNAs. **C,** Schematic presentation of *TAp63* transcript and *TAp63* reporters that carry TAp63 coding region alone, or together with TAp63 5′ or 3′UTR. Also shown below

is schematic presentation of GFP reporters that carry GFP coding region alone, or together with TAp63 5′UTR, 3′UTR, or a mutant 3′UTR with deletion of the putative IRE region. **D,** *IRP2*$^{-/-}$ MIA-PaCa2 cells were transfected with control pcDNA3 (−) or a vector expressing HA-IRP2 (+) along with a reporter that contains TAp63 coding region alone or together with TAp63 5′ or 3′UTR. Twenty-four hours posttransfection, cell lysates were collected and subjected to Western blot analysis to detect IRP2, TAp63 and actin. The level of proteins was normalized to that of actin, and the relative fold change is shown below each pair. **E,** Isogenic control (−) and *IRP2*-KO (+) MIA-PaCa2 cells were transfected with a reporter that contains GFP coding region alone or together with TAp63 5′ or 3′UTR. Twenty-four hours posttransfection, cell lysates were collected and subjected to Western blot analysis to detect IRP2, GFP, TAp63, and actin. The levels of GFP and TAp63 proteins were normalized to that of actin, and the relative fold change is shown below each pair. **F,** A putative IRE in *TP63* 3′UTR is recognized by and responsive to IRP2. *IRP2*$^{-/-}$ MIA-PaCa2 cells were transfected with control pcDNA3 (−) or a vector expressing HA-IRP2 (+) along with a GFP reporter as listed in **C**. Twenty-four hours posttransfection, cell lysates were collected and subjected to Western blot analysis to detect IRP2, GFP, TAp63, and actin proteins. The levels of GFP and TAp63 proteins were normalized to that of actin, and the relative fold change is shown below each pair.

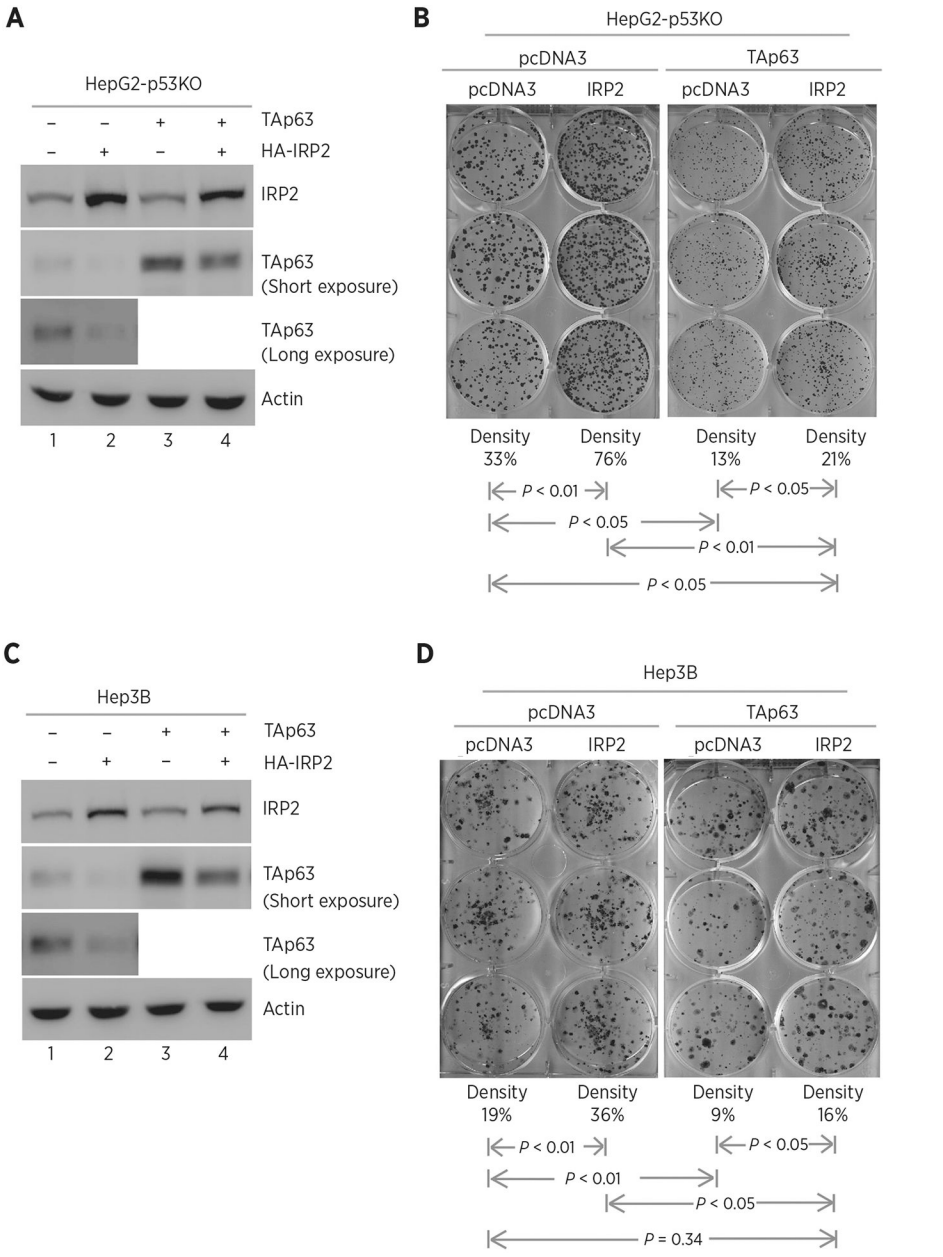

Figure 4.

Ectopic expression of *IRP2* promotes cell growth via TAp63. **A,** *p53*$^{-/-}$ HepG2 cells were transfected with control pcDNA3 or a vector expressing HA-tagged *IRP2* along with a control vector or a vector expressing *TAp63*. Twenty-four hours posttransfection, cell lysates were collected and subjected to Western blot analysis to detect IRP2, TAp63, and actin proteins. **B,** Colony formation assay was performed with *p53*$^{-/-}$ HepG2 cells transfected with control pcDNA3 or a vector expressing HA-tagged *IRP2*, followed by cotransfection with a control vector or a vector expressing *TAp63*. The relative density for colonies was showed below each image. **C** and **D,** The experiments were performed as in **A** and **B** except that *p53*$^{-/-}$ Hep3B cells were used.

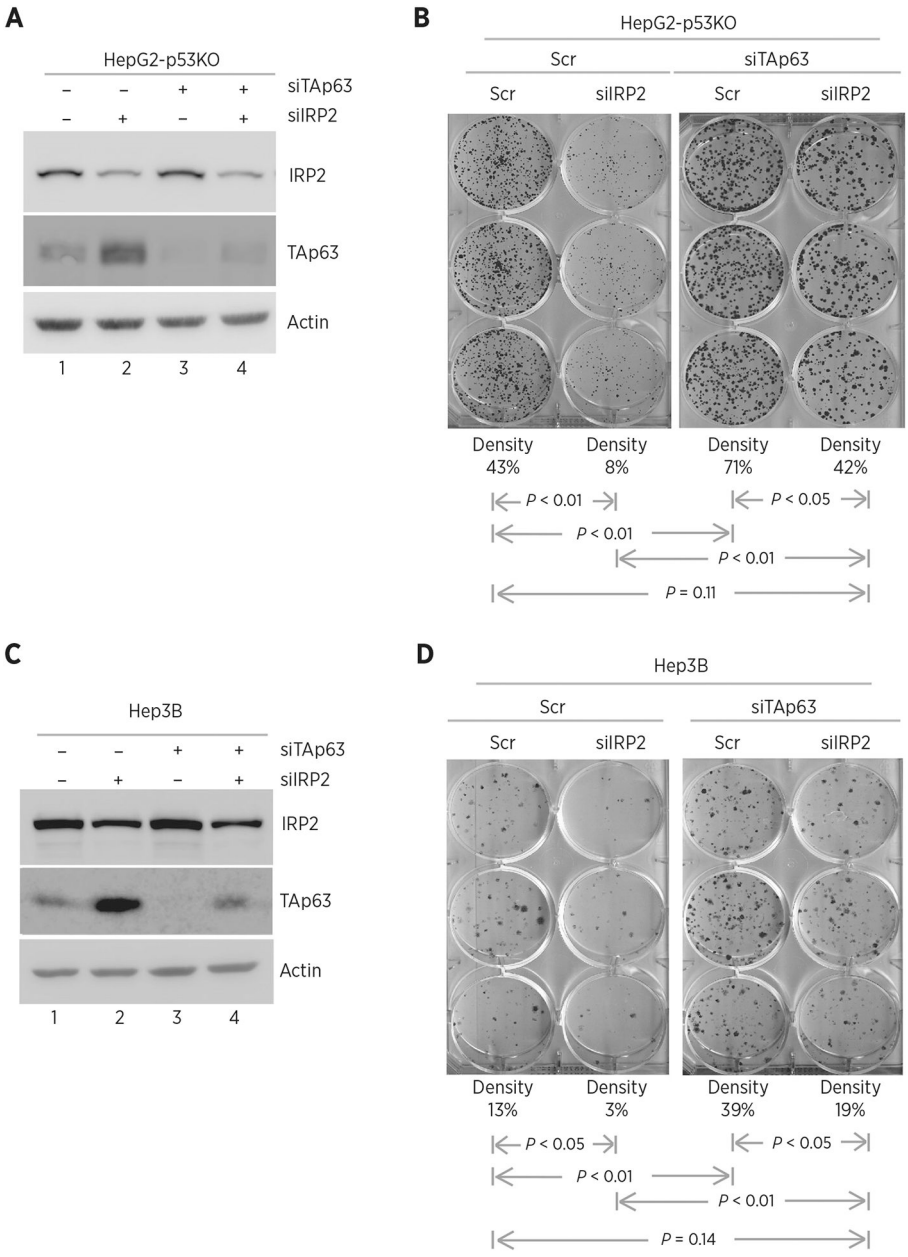

Figure 5.

Knockdown of *IRP2* inhibits cell growth via TAp63. **A,** *p53*$^{-/-}$ HepG2 cells were transfected with scrambled siRNA or siRNA against *IRP2*, followed by cotransfection with scrambled siRNA or siRNA against *TAp63* for 72 hours. Cell lysates were collected and subjected to Western blot analysis with various antibodies as indicated. **B,** Colony formation assay was performed with *p53*$^{-/-}$ HepG2 cells transfected with scrambled siRNA or siRNA against *IRP2*, followed by cotransfection with scramble siRNA or siRNA against *TAp63* for 72 hours. The relative density for colonies was showed below each image. **C** and **D,** The experiments were performed as in **A** and **B** except that *p53*$^{-/-}$ Hep3B cells were used.

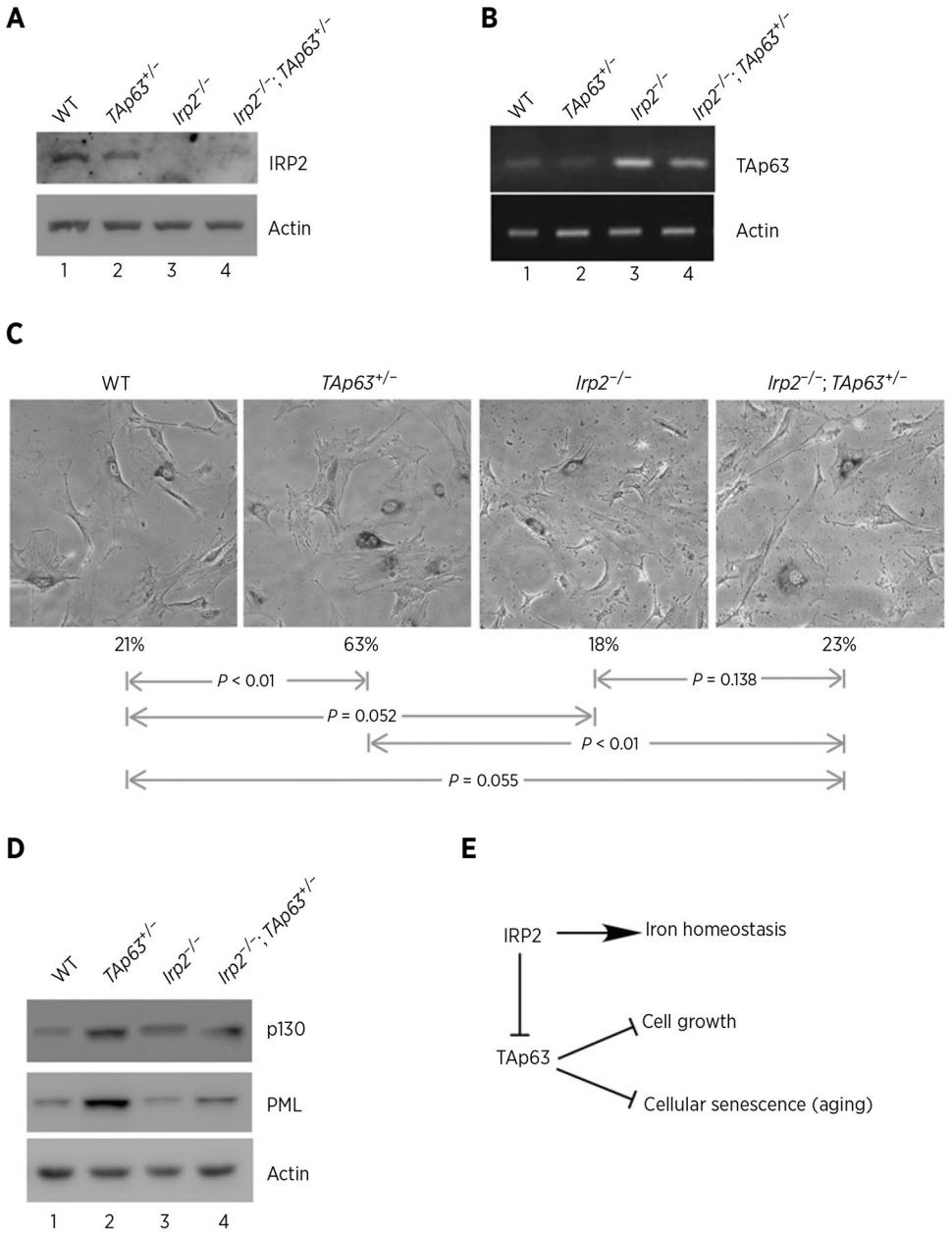

Figure 6.

Loss of *IRP2* inhibits cellular senescence induced by *TAp63* deficiency. **A,** Western blots were prepared using extracts from WT, *TAp63*$^{+/-}$, *Irp2*$^{-/-}$, and *Irp2*$^{-/-}$;*TAp63*$^{+/-}$ littermate MEFs. The blots were probed with antibodies against Irp2 and actin. **B,** The levels of *p63* and *actin* transcripts were measured in WT, *TAp63*$^{+/-}$, *Irp2*$^{-/-}$, and *Irp2*$^{-/-}$;*TAp63*$^{+/-}$ MEFs. **C,** Representative images of SA-β-Gal–stained WT, *TAp63*$^{+/-}$, *Irp2*$^{-/-}$, and *Irp2*$^{-/-}$;*TAp63*$^{+/-}$ MEFs. Quantification of the percentage of SA-β-Gal–positive cells was shown below each image. **D,** Western blots were prepared using extracts from WT, *TAp63*$^{+/-}$, *Irp2*$^{-/-}$, and *Irp2*$^{-/-}$;*TAp63*$^{+/-}$ MEFs. The blots were probed with antibodies

against p130, PML and actin, respectively. **E,** A model of how IRP2 modulates cell growth and cellular senescence via TAp63.